Ultrafast Excited State Dynamics in trans-N-Heterocyclic Carbene

Platinum(II) Acetylide Complexes

Silvano R. Valandro<sup>a,†</sup>, Ru He<sup>a,b,†</sup>, James D. Bullock<sup>b</sup>, Hadi Arman and Kirk S. Schanze<sup>a,\*</sup>

<sup>a</sup>Department of Chemistry, University of Texas at San Antonio, One UTSA Circle, San Antonio,

Texas 78249, United States

<sup>b</sup>Department of Chemistry, University of Florida, Gainesville, Florida 32611, United States

\* Corresponding author e-mail: kirk.schanze@utsa.edu

†Equal contributions

**Abstract** 

This study probes femto- and picosecond excited-state dynamics of a series of N-heterocyclic

carbene (NHC) ligand-containing platinum(II) complexes of the type trans-(NHC)<sub>2</sub>Pt<sup>II</sup>(CC-Ar)<sub>2</sub>,

where CC-Ar is an aryl acetylide. By using femtosecond transient absorption spectroscopy, two

dynamic processes are observed: an ultrafast singlet  $\rightarrow$  triplet intersystem crossing (< 0.3 ps),

followed by geometric/electronic relaxation that takes place on a 2-10 ps timescale. The

geometric/electronic relaxation is attributed to ligand torsional modes, mainly arising from

twisting of the aryl units relative to the square planar PtL<sub>4</sub> unit. The dynamics of this relaxation

process depend somewhat on steric constraints induced by substituent groups attached to the

(benzi)imidazole and phenyl ligands. The geometric relaxation dynamics slow with increasing

solvent viscosity. The experimental studies also reveal that the different conformers can be

photoselected by varying the excitation at different near-UV wavelengths. To corroborate the

experimental findings, density functional theory calculations (DFT) were conducted to probe the

effects of geometry and steric hindrance on the ground state energy surface. The calculations

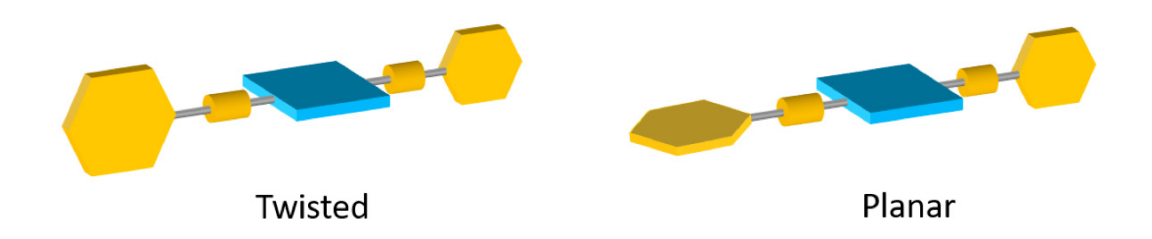
1

suggest that the barrier for torsion of the -CC-Ar units increases as N-substituents on the NHC ligands increase in order -CH $_3$  < -cyclohexyl < -n-butyl, and as the CC-Ar units are substituted in the 3,5-positions with *tert*-butyl groups.

## Introduction

Owing to their potential applications in organic light-emitting devices (OLED), Nheterocyclic carbene (NHC) based platinum(II) complexes have been the subject of intense research in the last decade. 1-13 These complexes display high phosphorescence emission efficiency in the blue and violet regions that is made possible by strong Pt(II)-induced spin-orbit coupling and strong σ-donating NHC ligands. Recently, our group has explored the optical properties of a series of trans-platinum(II) acetylide complexes featuring NHCs in both solution and solid state. 10, One feature that has emerged from this work is that the phosphorescence spectra of the complexes are influenced by emission from different conformers that are able to interconvert in fluid solution, but not in solid matrices at low temperature. 15, 18 Computational results indicate that in the ground-state torsional motion of the phenyl acetylide ligands is accompanied by a low energy barrier, and therefore they are essentially freely rotating in solution at room temperature.<sup>15</sup> This means that in the ground state, the energy difference between the twisted (T) and planar (P) conformations is small (Chart 1). In contrast, in the triplet excited state, the planar conformer is 10 kcal-mol<sup>-1</sup> or more lower in energy compared to the twisted conformer. The energy barrier in the triplet excited state for the torsion of both phenyl rings out of the plane relative to PtC4 is higher than 15 kcal mol. Thus, in the triplet state, one of the phenyl rings adopts the planar conformation, while the energy barrier for torsion of the other phenyl unit remains relatively low.<sup>15</sup> The T and P triplet-state conformers have different emission energies and spectra, and their ability to interconvert at low temperature in glassy solvents is inhibited by the rigidochromic effect. 19-20

Chart 1. Schematic showing structures of conformers of Pt-acetylide complexes. The blue square represents the square planar Pt complex and the yellow hexagons the phenyl acetylide units.



Understanding the excited state properties of these platinum-based triplet emitters is essential for their potential application in molecular optoelectronics. <sup>21</sup> The dynamics of the excited states in such systems play a vital role in controlling their optical properties. <sup>22</sup> In this context, in the present manuscript we report the application of ultrafast transient absorption spectroscopy to investigate the excited state relaxation dynamics that occur in *trans*-NHC Pt(II) acetylides. The compounds studied in this research are illustrated in Scheme 1.<sup>10, 14-15</sup> The overall objective of the present work is to understand the effects of sterics, solvent viscosity, and rigid media on the dynamics of conformational relaxation in the triplet excited states of these Pt(II) complexes. The results find that the *tert*-butyl substituents on the phenylene rings and n-butyl groups on the carbene ligands restrict the motion of the acetylide ligands, and this has an influence on the ultrafast dynamics. The effect of excitation wavelength in selective excitation of different populations of conformers is also explored. By changing the excitation wavelength, it is possible to photoselect different conformers, which gives rise to differences in excited state dynamics.

Scheme 1. Structure of trans-platinum(II) acetylides featuring N-heterocyclic carbenes.

## **Results**

Structures, Synthesis and Characterization. The study examined a matrix of four complexes that feature the general structure *trans*-(NHC)<sub>2</sub>Pt(CC-Ar)<sub>2</sub>. The NHC ligands used include a bis-cyclohexyl-substituted imidazole (Im) and bis-*n*-butyl substituted benzimidazole (Bim), while the aryl acetylide ligands include phenyl acetylene and bis-(*tert*-butyl)phenyl acetylene. The imidazole ligands were varied to examine the effect of the alkyl substituents and extended conjugation on the photophysics. The *tert*-butyl substituents were added to provide steric bulk on the phenyl acetylene units which was expected to influence their torsional dynamics.

Synthesis details for the *tert*-butyl substituted compounds, IPtP-*t*Bu and BiPtP-*t*Bu, are in the Supporting Information. The synthesis and characterization of the two other complexes (IPtP, BiPtP and IPtP-2) was reported previously. <sup>10, 14-15</sup> Structures of the complexes were confirmed by

<sup>1</sup>H NMR, <sup>13</sup>C NMR, and high-resolution mass spectrometry (see Supporting Information). The trans geometry of IPtP-*t*Bu and BiPtP-*t*Bu was confirmed by X-ray crystallography (Figure 1).

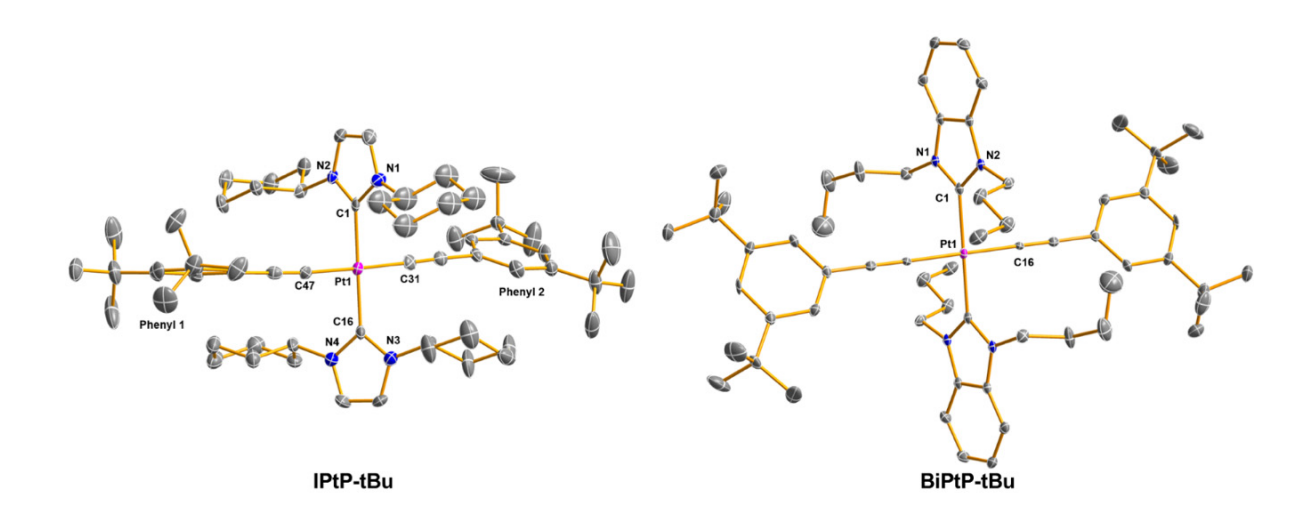


**Figure 1.** Crystal structures of complexes IPtP-*t*Bu and BiPtP-*t*Bu, with ellipsoids shown at the 50% probability level. Platinum atoms are shown in pink, nitrogen atoms are shown in blue and carbon atoms are shown in gray. Carbon-bound hydrogen atoms and solvent molecules are omitted for clarity.

The platinum atom sits on the inversion center of BiPtP-*t*Bu, while the crystal structure of IPtP-*t*Bu is not symmetric. BiPtP-*t*Bu features a Pt-carbene distance of 2.023(4) Å and the Pt-carbene distances of IPtP-*t*Bu are 2.013(6) Å (Pt1-C1) and 2.010(6) Å (Pt1-C16). These Pt-carbene distances are similar to those of previously reported *trans*-NHC Pt(II) acetylide complexes.<sup>10, 15</sup> The plane defined by the platinum atom and four carbon atoms connected to it is referred as the PtC<sub>4</sub> plane. For IPtP-*t*Bu, the dihedral angles between the phenyl rings and the PtC<sub>4</sub> plane are 85.561(4)° for Phenyl1 and 69.077(4)° for Phenyl2. The dihedral angle between the phenyl ring and PtC<sub>4</sub> plane of BiPtP-*t*Bu is 36.062(2)°, which is smaller than those of IPtP-*t*Bu. The two carbene ligands of IPtP-*t*Bu feature two different dihedral angles, N2-C1-N1 vs PtC<sub>4</sub> is

83.138(219)° and N4-C16-N3 vs PtC<sub>4</sub> is 64.830(191)°. The dihedral angle between the carbene ligand and PtC<sub>4</sub> of BiPtP-*t*Bu is 78.403(169)°.

Photophysical Properties. The UV-visible absorption and photoluminescence emission spectra of the complexes at room temperature are shown in Figure 2 and Figure S9 (Supporting Information). A summary of photophysical properties of the trans-NHC platinum acetylate complexes is given in Table 1. In general, the absorption of trans-NHC Pt(II) acetylides exhibit a strong electronic transition ( $\varepsilon > 3 \times 10^4 \, \text{M}^{-1} \, \text{cm}^{-1}$ ) in the near UV-region (Figure 2a). Based on the previous reports on trans-NHC Pt(II) acetylides, we attribute the strong absorption to a  $\pi$ - $\pi$ \* transition, where the frontier orbitals of these complexes are located primarily on the phenyl acetylide ligands and Pt metal center.<sup>10</sup> This assignment is supported by time-dependent density functional theory (TD-DFT) calculations carried out on IPtP (see supporting information). In particular, the strong near-UV transition is associated with a transition between orbitals with  $\pi$  and  $\pi$ \* character (HOMO)  $\rightarrow$  (LUMO + 2) (see Table S3 and Figs. S13 and S14). The trans-NHC platinum acetylate complexes bearing Bim ligands exhibit larger molar absorptivity compared to the Im analogues, due to the expanded  $\pi$ -system in the benzimidazole ring. <sup>15, 23</sup> The complexes containing tert-butyl groups (-tBu) on the phenyl acetylide ligands showed a slight decrease in long-wavelength absorption band (around 310-340 nm) compared to the unsubstituted phenyl acetylide platinum complexes. This slight spectral difference for the complexes containing -tBu ligands has been noted in other Pt(II) acetylide complexes had ascribed to a greater proportion of the twisted (Chart 1) conformers.<sup>24</sup>

The phosphorescence emission was measured in nitrogen bubble degassed THF at room temperature. All platinum (II) complexes featured a strong phosphorescence emission with a maximum in the range of 438 - 448 nm with a characteristic shoulder on the long wavelength side

(Figure 2b). The emission maxima of IPtP-tBu and BiPtP-tBu are bathochromically shifted 4 and 7 nm relative to IPtP and BiPtP, respectively. The long wavelength emission shoulders arise from vibrational coupling, and they notably become broader and more intense for IPtP-tBu and BiPtP-tBu. This effect may be due to due to emission from multiple unrelaxed excited state conformers. Compared to IPtP and BiPtP, -tBu-containing complexes display noticeably smaller phosphorescence quantum yields and longer lifetimes (Table 1). The smaller  $\Phi_{ph}$  and longer  $\tau_{ph}$  observed for IPtP-tBu and BiPtP-tBu are the result of a lower radiative decay rate compared to the unsubstituted phenyl analogs.

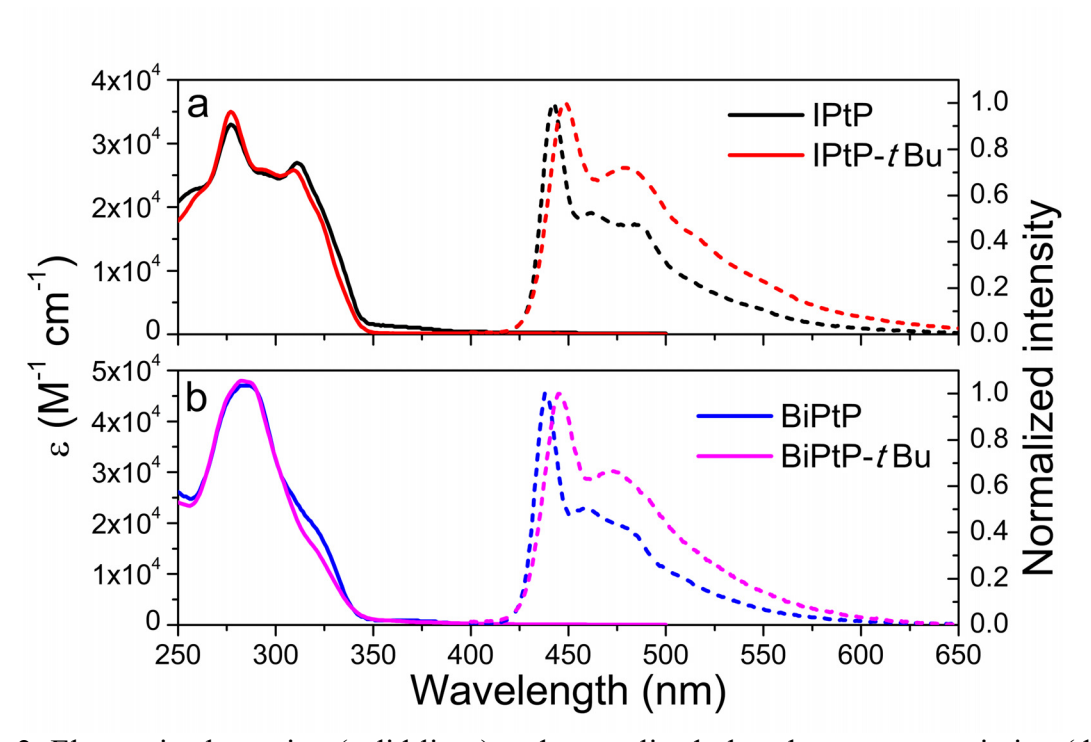


**Figure 2**. Electronic absorption (solid lines) and normalized phosphorescence emission (dashed lines) of (a) IPtP, IPtP-tBu, and (b) BiPtP and BiPtP-tBu in THF at room temperature,  $\lambda_{ex}$ =330 nm.

**Table 1**. Photophysical Properties of the Pt-complexes.

Compound	$\lambda_{\max}^{(abs)d}$		$\lambda_{max}^{(em)f}$	$\Phi_{ m ph}^g$	$ au_{ m ph}{}^h$	k <sub>r</sub>	k <sub>nr</sub>	Eem
	(nm)	$(M^{-1}cm^{-1})$	(nm)		(µs)	$(10^4  \mathrm{s}^{-1})$	$(10^5  \mathrm{s}^{-1})$	(eV)
IPtP <sup>a</sup>	279	33000	444	0.03	1.7	1.8	5.7	2.79
IPtP-tBu	279	35 000	448	0.02	2.5	0.93	3.9	2.77
$\mathrm{BiPtP}^b$	289	46 000	438	0.08	1.8	4.4	5.1	2.83
BiPtP-tBu	289	48 000	445	0.04	4.5	0.92	2.1	2.79
IPtP-2 <sup>c</sup>	357	83 000	531	0.54	575	-	-	-

<sup>&</sup>lt;sup>a</sup> Ref. <sup>10</sup>. <sup>b</sup> Ref. <sup>15</sup>. <sup>c</sup> Ref. <sup>14</sup>. <sup>d,e</sup> Measured in THF. <sup>f</sup> Measured in nitrogen bubble degassed THF. <sup>g</sup> Measured in nitrogen bubble degassed THF with respect to Ru(bpy)<sub>3</sub>Cl<sub>2</sub> ( $\Phi$  = 0.038) in aerated D.I. water. <sup>h</sup> Measured by TCSPC in bubble degassed THF solution.

Transient Absorption Spectroscopy. Femtosecond transient absorption measurements for IPtP, IPtP-tBu, BiPtP, and BiPtP-tBu in THF were carried out and are shown in Figure 3. Overall, promptly after 330 nm laser pulse excitation, a broad transient absorption band is observed with a shoulder around 500 - 550 nm and a maximum at 600 - 650 nm. For the Im complexes (Fig. 3a,b), this feature narrows down and increases in amplitude with a slight red-shift until roughly 30 ps. On the other hand, transient absorption spectra for Bim complexes (Fig. 3c,d) showed a more intense short wavelength shoulder, which increases in intensity with delay time in concert with the long-wavelength band at ~620 nm. Note that in general, the transient absorption amplitude at ~525 nm is more intense for -tBu substituted complexes containing groups. The transient absorption dynamics (Figure S10) were monitored for each complex at the maximum wavelength and fitted using multi-exponential functions. All complexes feature rising amplitude signals with ultrafast  $(\tau_1 = 0.2 - 0.3 \text{ ps})$  and fast  $(\tau_2 = 4 - 18 \text{ ps})$  components (Table 2). Note that the fast growth time constant  $\tau_2$  is generally larger for the Bim complexes, indicating a slower process. Another important observation concerns the relative amplitudes of the  $\tau_2$  component. In particular, it is evident that the relative amplitude for this component is larger for the Bim complexes, and generally smaller for the -tBu substituted complexes. Global analysis of the kinetics (see Supporting Information, Figure S11) reveals that the multiwavelength dynamics for all the complexes can be fit with two time constants, and the values are in agreement with the values present in Table 2.

In view of the general trends seen and previous work, it is likely that the ultrafast component  $(\tau_1)$  can be attributed to singlet-triplet intersystem crossing  $(k_{ISC} \approx 4 \text{ x } 10^{12} \text{ s}^{-1})$ , while the fast component  $(\tau_2)$  is due to conformational relaxations associated with the twisting of the phenyl acetylide ligands and/or carbene ligands in the triplet excited state. Note that the ultrafast intersystem crossing (ISC) rate is consistent with previously reported ISC rates for other platinum (II) complexes.

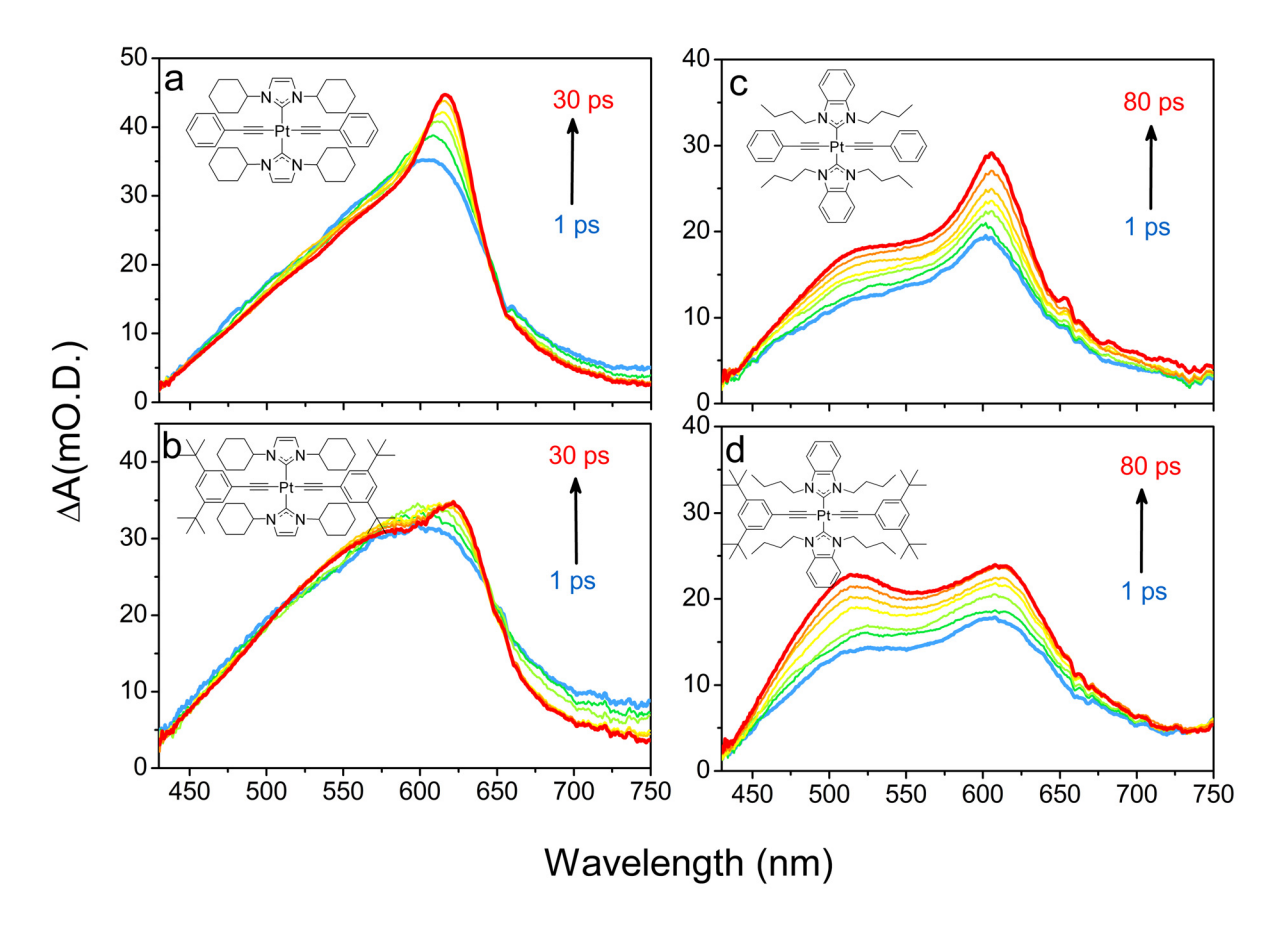


**Figure 3**. Ultrafast transient absorption spectra at various time delay for (a) IPtP, (b) IPtP-*t*Bu, (c) BiPtP and (d) BiPtP-*t*Bu in THF after excitation at 330 nm.

Table 2. Ultrafast transient absorption dynamics in THF <sup>a</sup>

Compound	τ <sub>1</sub> / ps	τ <sub>2</sub> / ps
IPtP	0.27±0.02 (0.85)	4.2±0.4 (0.15)
IPtP-tBu	$0.28 \pm 0.02 \ (0.94)$	4.6±0.7 (0.06)
BiPtP	$0.26\pm0.02~(0.56)$	17.8±0.3 (0.43)
BiPtP-tBu	$0.22 \pm 0.03 \ (0.74)$	11.2±0.3 (0.26)

<sup>&</sup>lt;sup>a</sup> Monitored at TA band maximum, 600 - 620 nm. Numbers in parenthesis are the normalized amplitudes of lifetime components. Inf = lifetime is too long to determine.

To obtain further insight into the motion of ligands during the excited state relaxation process, the TA dynamics for IPtP were measured in solvents of varying viscosity and in a poly(methyl methacrylate (PMMA) glass matrix. Tetraethylene glycol dimethyl ether (TEGDME) was chosen as solvent due to its high viscosity (3.335 mPa-s) compared to THF (0.481 mPa-s).  $^{27-28}$  By varying the ratio between THF and TEGDME the bulk solvent viscosity is varied and the corresponding dynamics of IPtP were collected, and the components associated to the triplet conformation relaxation are given in Table S1. Interestingly it is seen that the fast component ( $\tau_2$ ) becomes longer with increase in solvent viscosity up to THF/TEGDME (1:2) (Figure S12). This trend is consistent with assignment of this dynamic component to geometrical relaxation on the triplet excited state potential surface.

poly(Methyl methacrylate) (PMMA) glass monoliths that contain the *trans*-NHC platinum (II) acetylide complexes were prepared by *in situ* polymerization of methyl methacrylate and azoisobutyronitrile as described previously.<sup>29</sup> The transient absorption spectra of IPtP and BiPtP in these PMMA monoliths are shown in Figure 4. Interestingly, the spectra are quite similar to those for the same complexes in fluid solution, but the TA band maxima are slightly red-shifted and stimulated emission is observed below 500 nm. The time constants associated to the

conformation relaxation for IPtP and BiPtP in PMMA glass matrix were  $\tau_2 = 3.5$  ps and  $\tau_2 = 10.0$  ps, respectively.

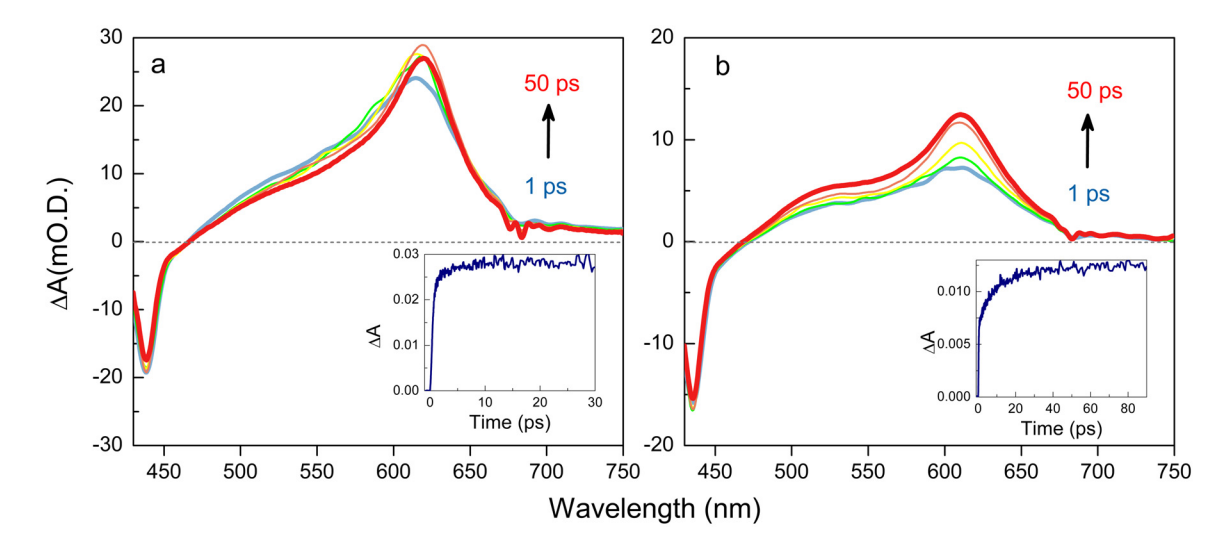


**Figure 4**. (a) Transient absorption spectra at various time delays of PMMA monolith doped with (a) IPtP and (b) BiPtP after excitation at 330 nm. Inset: kinetic trace at 620 nm for IPtP and 610 nm for BiPtP.

In a previous report we demonstrated photoselection of phosphorescence emission from non-equilibrating conformers of IPtP in a frozen solvent glass. Specifically, by exciting IPtP at short wavelength (278 nm), the phosphorescence emission spectrum was dominated by a progression with a high energy 0-0 band (417 nm). On the on the other hand, with excitation at longer wavelength (340 nm), the 0-0 emission band is shifted to a longer wavelength (439 nm). Thus, the conformers have different absorption spectra, and it is possible to selectively excite them. In order to explore this conformer photoselectivity and its effect on the conformational relaxation dynamics, we planned to study the effect of excitation wavelength on ultrafast transient absorption of IPtP. However, due to the limitation of the transient absorption system which cannot access the deep UV excitation below 300 nm, we decided to carry out excitation wavelength dependence measurements with IPtP-2, which has a red-shifted absorption compared to IPtP. The absorption

and emission spectra of this complex are given in Supporting Information. The selected excitation wavelengths used for the TA experiments with IPtP-2 were 330 nm and 370 nm.

Figure 5a shows the transient absorption spectra at different time delays for IPtP-2 in THF after 330 nm excitation. At early time delay of 1 ps, the transient absorption band is broad with a maximum at 565 nm and a shoulder at 515 nm. With increasing delay time (1-5 ps), the shoulder decays, and on a longer time scale an increase of a red-shifted band at 590 nm. This process can be assigned to ISC and the triplet relaxation as observed for IPtP. The overall dynamics (Figure 5c) of IPtP-2 at 600 nm were fitted with two components  $\tau_1 = 1.48$  ps and  $\tau_2 = 12.4$  ps. The transient absorption spectra for 370 nm excitation (Figure 5b) at the early time (1 ps) is similar to that of 330 nm excitation. However, the growth observed at 590 nm much less prominent in this case, and the dynamics could be fitted with one component with  $\tau = 1.11$  ps (Figure 5d). These results show quite clearly that the excitation wavelength has an influence on the spectral dynamics in IPtP-2; notably the amplitude of the slower phase, which is ascribed to conformational relaxation, is enhanced with the shorter wavelength excitation. This is consistent with the notion that short wavelength excitation photoselects conformers that are geometrically more distorted relative to the most stable triplet conformation, and thus greater spectral changes are seen during the relaxation phase following photoexcitation.

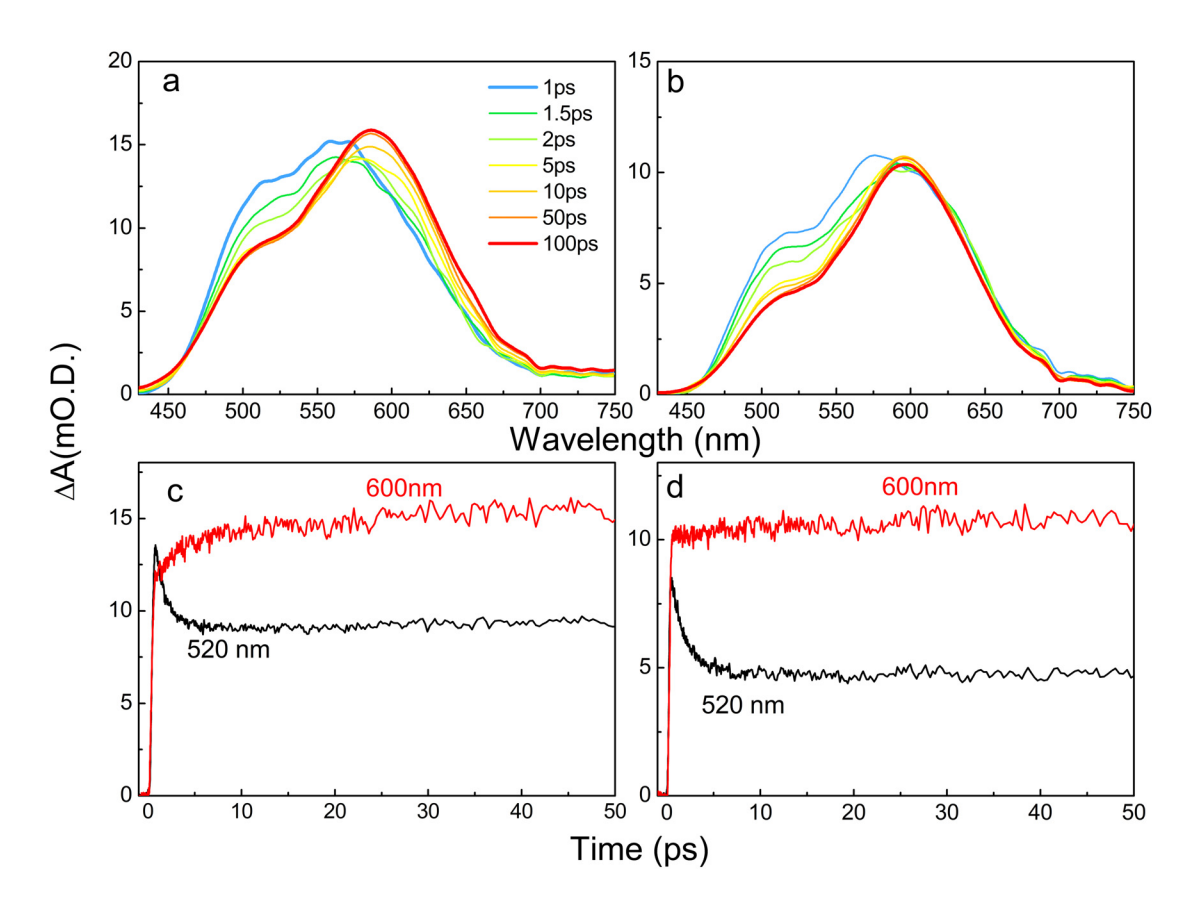


**Figure 5**. Transient absorption spectra at various time delays for IPtP-2 in THF after excitation at (a) 330 nm and (b) 370 nm. Kinetics trace monitored at 520 nm and 600 nm for IPtP-2 in THF after excitation at (c) 330 nm and (d) 370 nm.

Computational Investigations. We previously reported a study that applied density functional theory (DFT) calculations to explore the effect of conformation on the energy of the ground and triplet excited states of IPtP (except the alkyl groups on the NHC ligand were -CH<sub>3</sub>).<sup>15</sup> These calculations give several important conclusions. 1) In the ground state the energy barrier to torsion of the phenyl rings is low (~ 1 kcal-mol<sup>-1</sup>). 2) In the triplet state, one of the phenyl units is strongly constrained to remain in the planar (P) conformation with respect to the PtC<sub>4</sub> plane (Chart 1), with a barrier to twisting as high as 17 kcal-mol<sup>-1</sup>. This result was interpreted as indicating that the triplet excitation is localized strongly on a single -CC-Ph ligand that is conjugated with the

Pt(II) center, and the metal-ligand interaction is optimal with when the -CC-Ph ligand is in the P conformation.

In the current work we have expanded the DFT calculations with the aim to elucidate the effects of sterics on the energy of different torsional conformers. For expediency, these calculations were carried out on the ground state, with the assumption that the steric effects would carry over to the excited states. Detailed computational methods are given in the Experimental Section. In order to simplify the first series of calculations, the IPtP structure was used with the N-cyclohexyl groups on the NHC ligands replaced with methyl (-CH<sub>3</sub>) groups. At the start the dihedral angles between the planes of the two phenyl rings and the plane defined by PtC<sub>4</sub> (PtC<sub>4</sub> plane) were set to  $\theta = 30^{\circ}$  and  $\phi = -30^{\circ}$  (refer to Figure 6b) based on the calculated minimum ground state energy reported previously. <sup>15</sup> In addition, the dihedral angle between the imidazole rings and PtC<sub>4</sub> plane N1-C1-Pt1-C8 and N4-C14-Pt1-C19 were initially constrained to 90° and -90° (refer to Figure 6a). Then a scan was carried out while constraining one of the phenyl rings (φ = -30°) and conducting a relaxed torsional scan on the other phenyl ring ( $\theta = 30 - 200^{\circ}$ , see Fig. 6a,b). After the scan over  $\theta$ , the imidazole dihedral angle (N1-C1-C14-N4) was incremented down from 90° and new relaxed torsional scans were performed. This cycle was repeated until the imidazole dihedral reached 70°, and the resulting energies were used to construct the potential energy surface (PES) as a function of the phenyl ring torsional scan ( $\theta$ ) and the imidazole dihedral angle (Figure 6c).

Several features are apparent in these results. First, consistent with the findings reported previously, the PES is shallow with the energy difference between the global minimum and maximum conformers < 1 kcal-mol<sup>-1</sup>. Second, the energy is maximum when  $\theta$  is approximately  $70^{\circ}$  and decreases to a minimum when  $\theta \approx 170^{\circ}$ . These structures correspond approximately to the

twisted (T) and planar (P) phenyl conformers, respectively. Finally, decreasing the dihedral angle between the two imidazole rings leads to an increase in the energy barrier for phenyl torsion. This latter effect is not surprising and is likely due to increased steric interactions between the N-alkyl groups on the NHC ligands and the phenyl group.

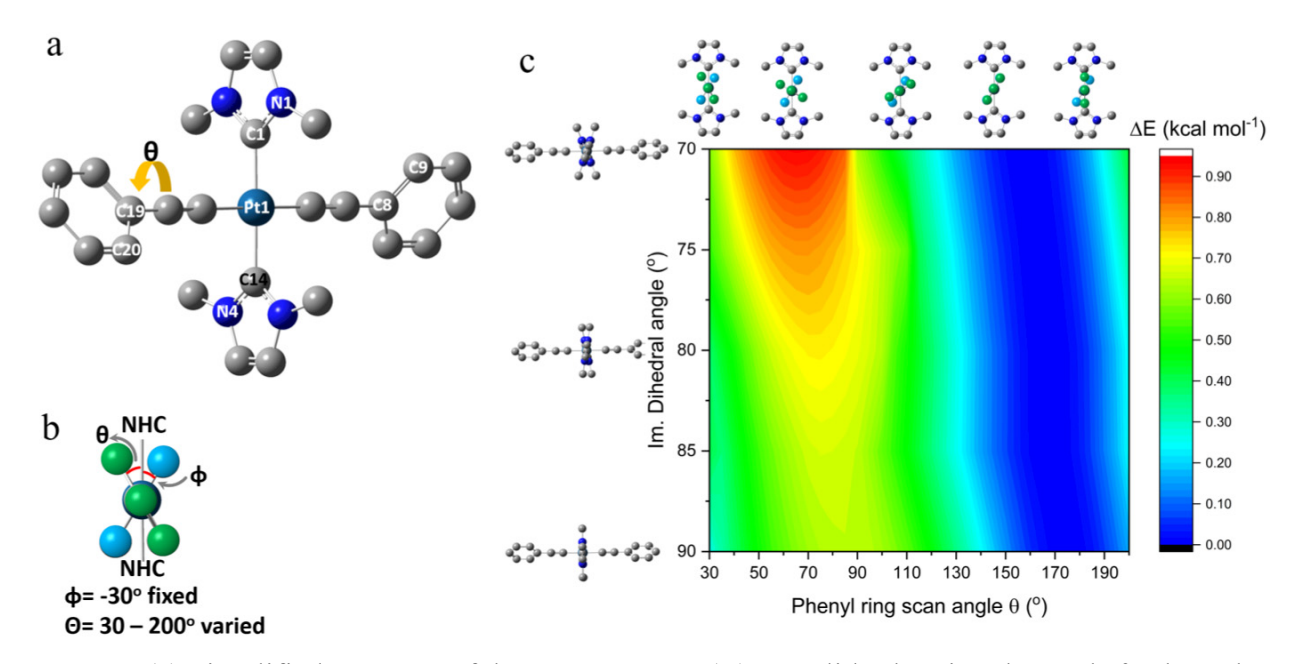


**Figure 6**. (a) Simplified structure of the *trans*-NHC Pt(II) acetylide showing the angle  $\theta$  where the relaxed torsional scan was applied, (b) Side view of the simplified structure showing the angles  $\theta$  and  $\phi$  and (c) Surface of the variation of energy barrier vs. the phenylene ring torsional scan vs the imidazole rings angle.

Based on the results from Figure 5a, we carried out the torsional scans for *trans*-NHC Pt(II) complexes with N-cyclohexyl or N-butyl substituents on the NHC ligands, or bis-3,5-t-Butyl substituents CC-phenyl ligands (see Fig. 7 for the structures used for each torsional scan). In these calculations, the NHC angles were constrained to  $80^{\circ}$  and relaxed torsional scans of one phenyl unit ( $\theta$ ) were conducted according to the same approach described above. As we can see in Figure 7a the torsional energy barrier increases as N-substituents on the imidazole ligands vary in the order -CH<sub>3</sub> < -cyclohexyl < -butyl. Similarly, the torsional barrier increases when t-Bu groups are

on the phenyl rings (Figure 7b). Taken together, the calculations show that in the ground state, the energetically more stable conformation is where the phenyls are in plane with PtC<sub>4</sub> (P conformer, Chart 1). However, the energetic cost for twisting is comparatively low, but it does increase as the steric bulk of the substituents on the imidazole and phenyls increases.

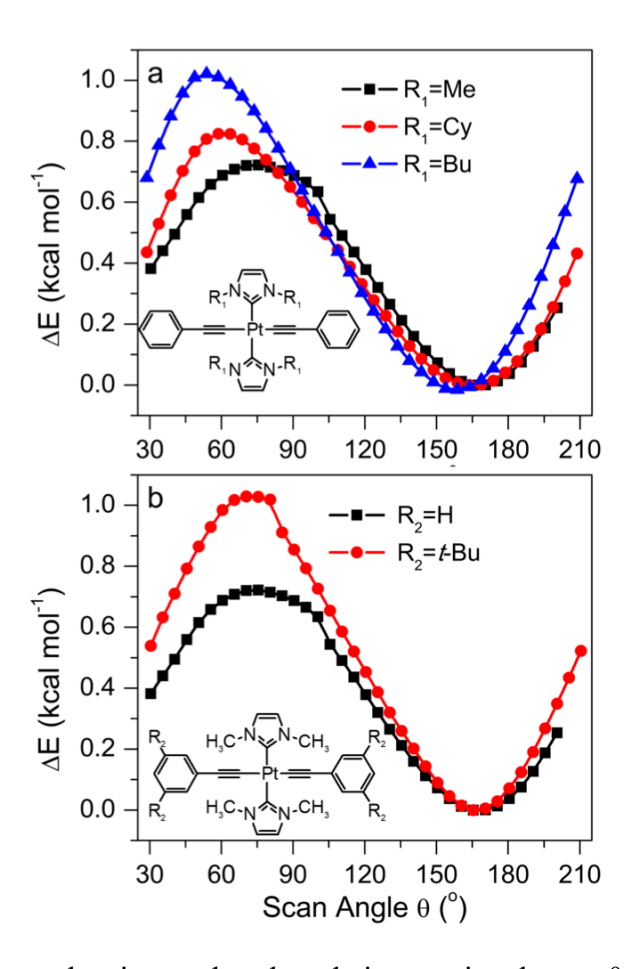
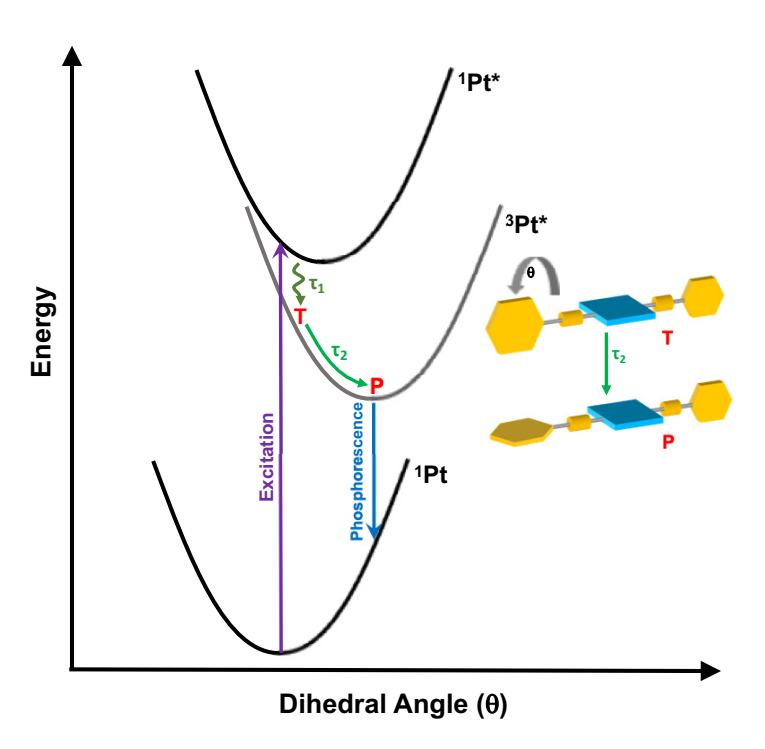


**Figure 7**. Variation of energy barrier vs the phenyl ring torsional scan  $\theta$  for trans-NHC Pt(II) acetylide containing (a) NHC ligands and (b) CC-phenyl ligands. In these plots, the P-conformation corresponds to 180°.

General Discussion. As noted in the introduction, in previous work on Pt-acetylide chromophores we have observed spectroscopic data that reveal the presence of different excited state conformers.<sup>15, 18</sup> The evidence points to involvement of torsional modes associated with twisting of the phenyl acetylide groups relative to the plane defined by the square planar PtL<sub>4</sub>

moiety. The goal of the study reported in this paper was to apply ultrafast transient absorption spectroscopy to probe the dynamics of conformational relaxation following photoexcitation of complexes of the type (NHC)<sub>2</sub>Pt(CC-Ar)<sub>2</sub>.

The ultrafast transient absorption results presented above (Fig. 3) demonstrate that in the excited-state these complexes feature two distinct dynamic processes that occur in the 200 fs – 20 ps timescale. One has a time constant  $\tau_1 \sim 250$  fs and it is attributed to  $S_1 \rightarrow T_1$  ISC. The second  $(\tau_2)$  is a slower component that occurs on the 4 – 18 ps timescale, that we attribute to being mainly due to conformational relaxation on the  $T_1$  energy surface (refer to Scheme 2). Given the results



**Scheme 2**. Qualitative energy diagram illustrating relaxation dynamics.

presented and discussed above it is reasonable to attribute this slower dynamic process to torsional motion of the phenyl units in the acetylide ligands. Several lines of reasoning lead to this conclusion. First, the relative amplitude of the  $\tau_2$  component is smaller for the *t*-Bu substituted complexes IPtP-*t*Bu and BiPtP-*t*Bu compared to their unsubstituted congeners (Table 2). The

reason for this is hypothesized to be due to the fact that for the *t*-Bu complexes the steric interactions give rise to a greater proportion of molecules in the P conformation in the ground state (Fig. 7b). Therefore, upon photoexcitation, more molecules will already be in the favored P conformation upon photoexcitation  $T_1$ , therefore fewer will undergo conformational relaxation. Second, it is found that the transient absorption spectra and dynamics for IPtP-2 exhibit a pronounced excitation wavelength dependence. Specifically, with longer wavelength excitation there is less spectral shift in the transient absorption with time, and the amplitude of the  $\tau_2$  component is substantially smaller. This is attributed to longer excitation wavelength photoselection of a sub-set of molecules that are in ground state conformations that are more closely aligned with the energetically-preferred P excited state conformation. While we associate the slower relaxation as being due to phenyl torsion, it is important to point out that there are other relaxation channels that may also contribute to the spectral dynamics occurring in the 5 – 20 ps timescale. These could include relaxation of hot vibrational states, relaxation of other torsional or other low frequency modes, as well as solvent relaxation dynamics.<sup>30</sup>

The solvent viscosity-dependent transient absorption experiments (THF/TEGDME mixtures) also support the hypothesis that the  $\tau_2$  component arises from a conformation change in  $T_1$  (Table S1, Fig. S11). In particular, as the fraction of the TEGDME increases, we observe a clear increase in the lifetime of the  $\tau_2$  component. It is well-established in the literature<sup>31-33</sup> that torsional dynamics in molecular chromophores slow with increasing solvent viscosity due to viscous friction. The timescale of the  $\tau_2$  component that we attribute to phenyl torsion is in a same range and varies by a similar amount with viscosity compared to excited state torsional motion of *trans*-stilbene and biphenyls.<sup>34-37</sup>

Finally, we were confused by the results in the PMMA matrix where the dynamics of the  $\tau_2$  phase are seemingly unaffected by the glassy environment. In this case we hypothesize that the relaxation is associated with molecules that are in polymer environments where there is sufficient free volume to allow the rotation of the phenyl to proceed with the same dynamics as observed in fluid solution. Similar observations have been made with molecular rotors in constrained environments such as polymers and in porous solid materials.<sup>38-40</sup> In essence, the phenyl units are likely able to freely rotate in polymer environments where the free volume is sufficient to allow unconstrained molecular rotor type motion to occur.

# **Summary and Conclusions**

In this work, we have presented a direct observation of phenyl rings relaxation dynamics from a twisted to a planar conformation of excited N-heterocyclic carbenes based platinum (II) complexes. The effect of side groups attached to the (benzi)imidazole and phenyl ligands have been studied by ultrafast transient absorption spectroscopy and computational methods. The NHC Pt(II) complexes featured a ultrafast rising component ( $\tau_1 = 0.2 - 0.3$  ps) apart with slower component. While the first one was attributed to  $S_1 \rightarrow T_1$  ISC, the second component with decay constant  $\approx 4 - 18$  ps was assigned to the torsional motion of the phenyl ring. Our computational analysis showed that the energy barrier for the torsional motion of one phenyl ring increases with the steric bulk of ligand substituent groups and matched our experimental observation. We also showed by excitation at different wavelengths it is possible to selectively excite distinct conformers leading to changes in the dynamics associated with the conformational relaxation.

## **Experimental**

**Synthesis and structure**. Details on the synthesis and structural characterization of IPtP-*t*Bu and BiPtP-*t*Bu are given in the Supporting Information.

Photophysical Measurements. UV-visible absorption spectra were obtained on a Shimadzu UV-1800 dual beam spectrophotometer. Steady state photoluminescence measurements were performed on an F1000 Edinburg spectrophotometer. Phosphorescence lifetime measurements were accomplished with a PicoQuant FluoTime 300 Fluorescence Lifetime Spectrophotometer by time-correlated single photon counting (TCSPC) technique (PicoQuant Time Harp module). In this system, a Ti:Saphire Coherent Chameleon Ultra laser was used as excitation source. The Chameleon laser provides pulses of 80 MHz that can be tuned from 680-1080 nm. The 80 MHz pulse train was sampled using a Coherent Model 9200 pulse picker to provide excitation pulses at an acceptable repetition rate and was frequency doubled using a Coherent second harmonic generator. An excitation wavelength of 330 nm was chosen for all samples. Femtosecond timeresolved transient absorption spectroscopy (fs-TA) measurements were performed using a broadband (350-1600 nm) pump-probe femtosecond transient absorption spectrometer HELIOS, Ultrafast Systems equipped with visible detector. An amplified femtosecond Ti:sapphire laser system (Astrella, Coherent, Inc.) displaying at 800nm with pulse width 100 fs and 1 kHz repetition rate coupled with an optical paramagnetic amplifier (Coherent) was used for pulse pump generation. Probe light in the visible and near-infrared was generated by passing a small portion of the 800 nm light from Ti:sapphire laser through a computerized optical delay and focusing in a sapphire plate to generate white-light continuum (VIS). The sample solutions were constantly stirred to avoid photodegradation. Theoretical calculations on NHC Pt(II) acetylides were performed using DFT in Gaussian 16, using the B3LYP functionality with the SDD basis set.

### **Acknowledgments**

We acknowledge the National Science Foundation for support of this work (Grant No. CHE-1904288).

# **Supporting Information**

The Supporting Information is available free of charge at http://www.acs.org.

Complete details concerning the synthesis and characterization of all new compounds, NMR spectra, X-ray crystallography summary table and additional photophysical results.

Crystallographic data of IPtP-*t*Bu

Crystallographic data of BiPtP-tBu

Results of DFT/TD-DFT Calculations: Frontier orbital plots, calculated absorption spectrum, TD-DFT calculated transitions.

#### References

- (1) Unger, Y.; Zeller, A.; Ahrens, S.; Strassner, T. Blue Phosphorescent Emitters: New N-Heterocyclic Platinum(II) Tetracarbene Complexes. *Chem. Commun.* **2008**, 3263-3265.
- (2) Unger, Y.; Zeller, A.; Taige, M. A.; Strassner, T. Near-UV Phosphorescent Emitters: N-heterocyclic Platinum(II) Tetracarbene Complexes. *Dalton Trans.* **2009**, 4786-4794.
- (3) Unger, Y.; Meyer, D.; Molt, O.; Schildknecht, C.; Munster, I.; Wagenblast, G.; Strassner, T. Green–Blue Emitters: NHC-Based Cyclometalated [Pt(C^C\*)(acac)] Complexes. *Angew. Chem. Inter. Edit.* **2010**, *49*, 10214-10216.
- (4) Hudson, Z. M.; Sun, C.; Helander, M. G.; Chang, Y. L.; Lu, Z. H.; Wang, S. Highly Efficient Blue Phosphorescence from Triarylboron-Functionalized Platinum(II) Complexes of N-Heterocyclic Carbenes. *J. Am. Chem. Soc.* **2012**, *134*, 13930-13933.
- (5) Li, K.; Cheng, G.; Ma, C. S.; Guan, X. G.; Kwok, W. M.; Chen, Y.; Lu, W.; Che, C. M. Light-Emitting Platinum(II) Complexes Supported by Tetradentate Dianionic bis(N-Heterocyclic Carbene) Ligands: Towards Robust Blue Electrophosphors. *Chem. Sci.* 2013, 4, 2630-2644.

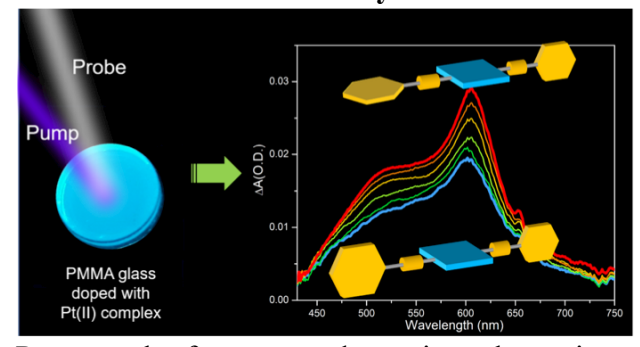
- (6) Zhang, Y. Z.; Blacque, O.; Venkatesan, K. Highly Efficient Deep-Blue Emitters Based on cis and trans N-Heterocyclic Carbene Pt-II Acetylide Complexes: Synthesis, Photophysical Properties, and Mechanistic Studies. *Chem.-Eur. J.* 2013, 19, 15689-15701.
- (7) Bachmann, M.; Suter, D.; Blacque, O.; Venkatesan, K. Tunable and Efficient White Light Phosphorescent Emission Based on Single Component N-Heterocyclic Carbene Platinum(II) Complexes. *Inorg. Chem.* 2016, 55, 4733-4745.
- (8) Luo, Y. F.; Xu, Y. Y.; Zhang, W. T.; Li, W. Q.; Li, M.; He, R. X.; Shen, W. Theoretical Insights into the Phosphorescence Quantum Yields of Cyclometalated (C boolean AND C\*) Platinum(II) NHC Complexes: pi-Conjugation Controls the Radiative and Nonradiative Decay Processes. J. Phys. Chem. C 2016, 120, 3462-3471.
- (9) Strassner, T. Phosphorescent Platinum(II) Complexes with C^C\* Cyclometalated NHC Ligands. *Acc. Chem. Res.* **2016**, *49*, 2680-2689.
- (10) Bullock, J. D.; Salehi, A.; Zeman, C. J.; Abboud, K. A.; So, F.; Schanze, K. S. In Search of Deeper Blues: Trans-N-Heterocyclic Carbene Platinum Phenylacetylide as a Dopant for Phosphorescent OLEDs. *ACS Appl. Mater. Interfaces* **2017**, *9*, 41111-41114.
- (11) Suter, D.; van Summeren, L. T. C. G.; Blacque, O.; Venkatesan, K. Highly Stable and Strongly Emitting N-Heterocyclic Carbene Platinum(II) Biaryl Complexes. *Inorg. Chem.* **2018**, *57*, 8160-8168.
- (12) Lee, J.-H.; Chen, C.-H.; Lee, P.-H.; Lin, H.-Y.; Leung, M.-k.; Chiu, T.-L.; Lin, C.-F. Blue Organic Light-Emitting Diodes: Current Status, Challenges, and Future Outlook. *J. Mater. Chem. C* 2019, 7, 5874-5888.
- (13) Li, G.; Zhao, X.; Fleetham, T.; Chen, Q.; Zhan, F.; Zheng, J.; Yang, Y.-F.; Lou, W.; Yang, Y.; Fang, K.; Shao, Z.; Zhang, Q.; She, Y. Tetradentate Platinum(II) Complexes for Highly Efficient Phosphorescent Emitters and Sky Blue OLEDs. *Chem. Mater.* **2020**, *32*, 537-548.
- (14) Winkel, R. W.; Dubinina, G. G.; Abboud, K. A.; Schanze, K. S. Photophysical Properties of trans-Platinum Acetylide Complexes Featuring N-Heterocyclic Carbene Ligands. *Dalton Trans.* **2014**, *43*, 17712-17720.
- (15) Bullock, J. D.; Valandro, S. R.; Sulicz, A. N.; Zeman, C. J.; Abboud, K. A.; Schanze, K. S. Blue Phosphorescent trans-N-Heterocyclic Carbene Platinum Acetylides: Dependence on Energy Gap and Conformation. *J. Phys. Chem. A* **2019**, *123*, 9069-9078.

- (16) Bullock, J. D.; Xu, Z. T.; Valandro, S.; Younus, M.; Xue, J. G.; Schanze, K. S. trans-N-(Heterocyclic Carbene) Platinum(II) Acetylide Chromophores as Phosphors for OLED Applications. *ACS Appl. Electron. Mater.* **2020**, *2*, 1026-1034.
- (17) He, R.; Xu, Z.; Valandro, S.; Arman, H. D.; Xue, J.; Schanze, K. S. High-Purity and Saturated Deep-Blue Luminescence from trans-NHC Platinum(II) Butadiyne Complexes: Properties and Organic Light Emitting Diode Application. *ACS Appl. Mater. Interfaces* **2021**, *13*, 5327-5337.
- (18) Glusac, K.; Kose, M. E.; Jiang, H.; Schanze, K. S. Triplet excited state in platinum-acetylide oligomers: Triplet localization and effects of conformation. *J. Phys. Chem. B* **2007**, *111*, 929-940.
- (19) Kotch, T. G.; Lees, A. J.; Fuerniss, S. J.; Papathomas, K. I.; Snyder, R. W. Luminescence Rigidochromism of Fac-Clre(Co)3(4,7-Ph2phen) (4,7-Ph2phen = 4,7-Diphenyl-1,10-Phenanthroline) as a Spectroscopic Probe in Monitoring Polymerization of Photosensitive Thin-Films. *Inorg. Chem.* **1993**, *32*, 2570-2575.
- (20) Lees, A. J. The Luminescence Rigidochromic Effect Exhibited by Organometallic Complexes: Rationale and Applications. *Comment. Inorg. Chem.* **1995**, *17*, 319-346.
- (21) Zhong, F. F.; Zhao, J. Z.; Hayvali, M.; Elmali, A.; Karatay, A. Effect of Molecular Conformation Restriction on the Photophysical Properties of N N Platinum(II) Bis(ethynylnaphthalimide) Complexes Showing Close-Lying (MLCT)-M-3 and (LE)-L-3 Excited States. *Inorg. Chem.* **2019**, *58*, 1850-1861.
- (22) Sheng, C. X.; Singh, S.; Gambetta, A.; Drori, T.; Tong, M.; Tretiak, S.; Vardeny, Z. V. Ultrafast Intersystem-Crossing in Platinum Containing π-Conjugated Polymers with Tunable Spin-Orbit Coupling. *Sci. Rep-UK* **2013**, *3*, 2653.
- (23) Barbante, G. J.; Francis, P. S.; Hogan, C. F.; Kheradmand, P. R.; Wilson, D. J.; Barnard, P. J. Electrochemiluminescent Ruthenium(II) N-Heterocyclic Carbene Complexes: a Combined Experimental and Theoretical Study. *Inorg. Chem.* **2013**, *52*, 7448-7459.
- (24) Lin, C. J.; Chen, C. Y.; Kundu, S. K.; Yang, J. S. Unichromophoric Platinum-Acetylides that Contain Pentiptycene Scaffolds: Torsion-Induced Dual Emission and Steric Shielding of Dynamic Quenching. *Inorg. Chem.* **2014**, *53*, 737-745.

- (25) Ramakrishna, G.; Goodson, T.; Rogers-Haley, J. E.; Cooper, T. M.; McLean, D. G.; Urbas, A. Ultrafast Intersystem Crossing: Excited State Dynamics of Platinum Acetylide Complexes. J. Phys. Chem. C 2009, 113, 1060-1066.
- (26) van der Veen, R. M.; Cannizzo, A.; van Mourik, F.; Vlcek, A.; Chergui, M. Vibrational Relaxation and Intersystem Crossing of Binuclear Metal Complexes in Solution. *J. Am. Chem. Soc.* **2011**, *133*, 305-315.
- (27) Aminabhavi, T. M.; Gopalakrishna, B. Density, Viscosity, Refractive Index, and Speed of Sound in Aqueous Mixtures of N,N-Dimethylformamide, Dimethyl Sulfoxide, N,N-Dimethylacetamide, Acetonitrile, Ethylene Glycol, Diethylene Glycol, 1,4-Dioxane, Tetrahydrofuran, 2-Methoxyethanol, and 2-Ethoxyethanol at 298.15 K. *J. Chem. Eng. Data* 1995, 40, 856-861.
- (28) Carvalho, P. J.; Fonseca, C. H. G.; Moita, M. L. C. J.; Santos, A. F. S.; Coutinho, J. A. P. Thermophysical Properties of Glycols and Glymes. *J. Chem. Eng. Data* **2015**, *60*, 3721-3737.
- (29) Price, R. S.; Dubinina, G.; Wicks, G.; Drobizhev, M.; Rebane, A.; Schanze, K. S. Polymer Monoliths Containing Two-Photon Absorbing Phenylenevinylene Platinum(II) Acetylide Chromophores for Optical Power Limiting. ACS Appl. Mater. Interfaces 2015, 7, 10795-10805.
- (30) McCusker, J. K.; Vlcek, A. Ultrafast Excited-State Processes in Inorganic Systems. *Accounts Chem. Res.* **2015**, *48*, 1207-1208.
- (31) Heisler, I. A.; Kondo, M.; Meech, S. R. Reactive Dynamics in Confined Liquids: Ultrafast Torsional Dynamics of Auramine O in Nanoconfined Water in Aerosol OT Reverse Micelles. *J. Phys. Chem. B* **2009**, *113*, 1623-1631.
- (32) Verolet, Q.; Rosspeintner, A.; Soleimanpour, S.; Sakai, N.; Vauthey, E.; Matile, S. Turn-On Sulfide pi Donors: An Ultrafast Push for Twisted Mechanophores. *J. Am. Chem. Soc.* **2015**, *137*, 15644-15647.
- (33) Ghosh, R.; Nandi, A.; Kushwaha, A.; Das, D. Ultrafast Conformational Relaxation Dynamics in Anthryl-9-benzothiazole: Dynamic Planarization Driven Delocalization and Protonation-Induced Twisting Dynamics. *J. Phys. Chem. B* **2019**, *123*, 5307-5315.
- (34) Saltiel, J.; D'Agostino, J. T. Separation of Viscosity and Temperature Effects on the Singlet Pathway to Stilbene Photoisomerization. *J. Am. Chem. Soc.* **1972**, *94*, 6445-6456.

- (35) Rothenberger, G.; Negus, D. K.; Hochstrasser, R. M. Solvent Influence on Photo-Isomerization Dynamics. *J. Chem. Phys.* **1983**, *79*, 5360-5367.
- (36) Courtney, S. H.; Fleming, G. R. Photoisomerization of Stilbene in Low Viscosity Solvents Comparison of Isolated and Solvated Molecules. *J. Chem. Phys.* **1985**, *83*, 215-222.
- (37) Liu, K. L.; Lee, S. J.; Chen, I. C.; Hsu, C. P.; Yeh, M. Y.; Luh, T. Y. Excited-State Dynamics of [(1,1 '-Biphenyl)-4,4-diyldi-2,1-ethenediyl]bis(dimethylsilane). *J. Phys. Chem. A* **2009**, 113, 1218-1224.
- (38) Loutfy, R. O. Effect of Polystyrene Molecular-Weight on the Fluorescence of Molecular Rotors. *Macromolecules* **1983**, *16*, 678-680.
- (39) Comotti, A.; Bracco, S.; Sozzani, P. Molecular Rotors Built in Porous Materials. *Accounts Chem. Res.* **2016**, *49*, 1701-1710.
- (40) Roy, K.; Kayal, S.; Ravi Kumar, V.; Beeby, A.; Ariese, F.; Umapathy, S. Understanding Ultrafast Dynamics of Conformation Specific Photo-Excitation: A Femtosecond Transient Absorption and Ultrafast Raman Loss Study. *J. Phys. Chem. A* **2017**, *121*, 6538-6546.

# For Table of Contents Only



Pump-probe femtosecond transient absorption spectroscopy was used to study the excited-state dynamics of a series of *N*-heterocyclic carbene (NHC) ligand-containing platinum(II) complexes of the type trans-(NHC)<sub>2</sub>Pt<sup>II</sup>(CC-Ar)<sub>2</sub>, where CC-Ar is an aryl acetylide. An ultrafast singlet  $\rightarrow$  triplet intersystem crossing, followed by a slower geometric/electronic relaxation were observed. The geometric/electronic relaxation is attributed to ligand torsional modes, mainly arising from twisting of the aryl units relative to the square planar PtL<sub>4</sub> unit.